Available online www.jsaer.com

***Journal of Scientific and Engineering Research*, 2020, 7(11):110-124**

Research Article

ISSN: 2394-2630
CODEN(USA): JSERBR

Comparative study of the models of the photovoltaic cell (1 diode & 2 diode) and efficiency optimization

Nabil Alkassoum[2], Boureima Seibou[1], Ousmane Mahamadou[1], Noma Talibi Soumaïla[2]*

[1]Electrical Engineering Department, Mines, Industry and Geology School, Niamey, Niger
[2]Laboratory of Energy, Electronics, Electrotechnics, Automatics and Industrial Computing, Abdou Moumouni University (UAM), Niamey, Niger

Abstract In this paper theoretical study of photovoltaic cell is made. Several single diode and two diode models have been described, modelled in MATLAB/SIMULINK and simulated. Effects of temperature and irradiation on the cell were particularly evident on the power, voltage and current of photovoltaic cell. Considering the poor adaptation of the operating point of the load of the photovoltaic system we had shown the interest of an adaptation stage. Adaptation stage used is composed of MPPT controlled Boost chopper and pulse width modulation (PWM). The modelling and simulation of the system (photovoltaic generator, Boost chopper, Pulse Width Modulation as well as the MPPT algorithm) is then carried out using the Matlab/Simulink software. Simulation results presented.

Keywords Modeling, photovoltaic cell; MPPT; Boost; optimization; MLI

Introduction

Situation of contemporary energy has favored development of new energies such as solar thermal and photovoltaic. For its photovoltaic operation, photovoltaic cells convert solar radiation directly into electricity. These are components based on extrinsic semiconductors of the P and N types [1-4].

These photovoltaic (PV) systems have low conversion rate and low power, optimal choice must be made. Photopiles are combined in series and in parallel to obtain usable powers. To verify their behavior under various conditions, models are used, several of which are available in the literature [2-4].

Materials used have wide diversity in terms of radiation absorption, energy conversion efficiency, technology and manufacturing cost. Different kinds of crystalline materials such as monocrystalline, polycrystalline and thin films are available [2, 5-6].

Solar cell provides electrical power depending on sunlight, temperature and daily and seasonal fluctuations. Photovoltaic cell can only provide maximum power for a specific voltage and current; this operation at maximum power depends on the load at its terminals. A device will be integrated into system to operate it at its maximum power, this device is MPPT controller [5-6].

Objective of this article is on one hand to make presentation of different models of photovoltaic cell. On other hand, to highlight the interest of using optimization device in photovoltaic system.

2. Principles and operations of the photovoltaic cell

A photovoltaic cell is PN semiconductor device that produces an electric current when exposed to light radiation [1, 4].

Two metal conductors in contact on both sides of the PV cell (Figure 1.b), allow the flow of electrical current. Thus, when photons are absorbed by semiconductor atoms, electrons are released from the negative zone. These electrons are collected by the metal conductors and circulate in the external circuit to reach the positive zone

thus creating an electric current from the positive zone to the negative (Figure 1.b)[1, 3, 5, 6]. These cells generate voltage ranging from 0.5 to 0.8 Volts depending on semiconductor used and manufacturing technology. Since the cell voltage is low, several cells will be connected in series and/or in parallel to achieve usable voltages and currents [1, 5, 6].

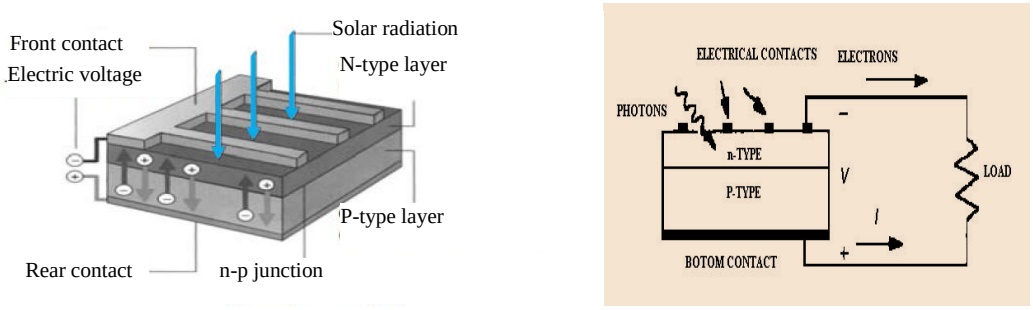

Figure 1: Photovoltaic cell: a) Schematic of the structure; b) Principle of photo-current

3. Photovoltaic cell performance.

3.1. Characteristics of the photovoltaic cell.

The main characteristics of the cell are:

1. Short-circuit current Isc (open circuit); current is at its maximum.
2. Open circuit voltage Voc (short-circuited circuit); voltage is at its maximum.
3. Maximum power or MPP (Maximal Power Point); defined by Imp current and Vmp voltage.

PV cell reaches its maximum value at the point (Vmp, Imp) (Figure 2). These values, Vmp and Imp are always given by the PV module manufacturer.

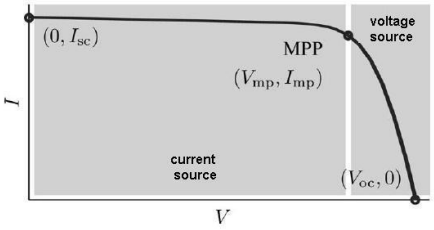

Figure 2: IV characteristics of PV panel

The characteristics of photovoltaic modules are given under the following conditions:

- STC (Standard Test Conditions): 1000 W/m^2 solar irradiance, 25°C cell junction temperature, and 1.5 AM solar spectrum.
- NOCT: (Nominal Operating Cell Temperature) is the junction temperature of the cell, it characterizes the thermal functioning of the module: it corresponds to the temperature for a solar irradiance of 800 W/m^2, an ambient temperature of 20°C and an average wind speed of 1 m/s.

3.2. Effects of irradiation and temperature variation on the photopile

a) Irradiation effect of change in on current-voltage characteristic of PV module

Figure (3.a) shows that when irradiation increases, short-circuit current increases faster than open loop voltage and maximum power increases.

On other hand, Figure 3.b shows decrease in current and voltage as function of temperature. Current changes more slowly than voltage.

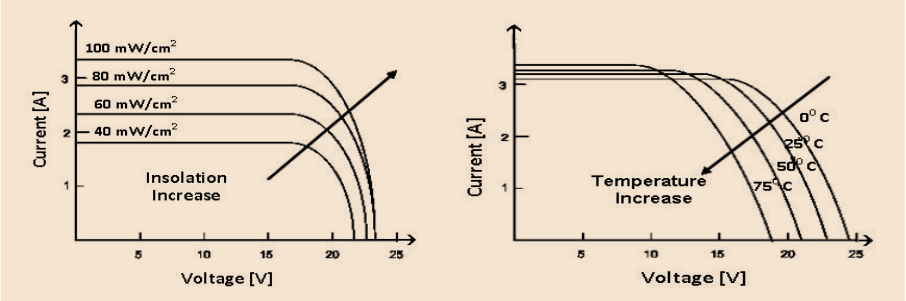

a b

Figure 3: Caractéristique IV de la cellule PV : a) en fonction de l'irradiation ; b) en fonction de la température.

Maximum MPP power point is constantly changing, taking into account influence of temperature and irradiation on operation of PV module, (Figure 4).

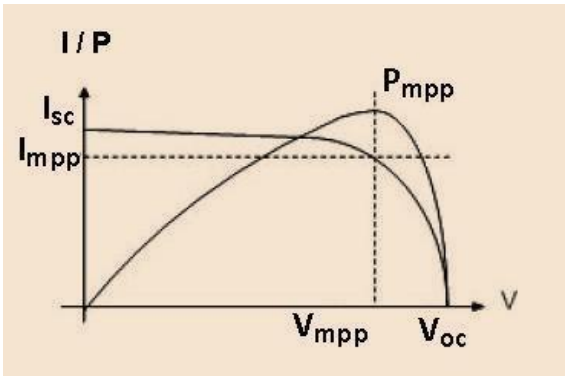

Figure 4: Characteristics IV and P-V of the PV cell with MPP

4. Methodology

Modelling is the basis for simulating real systems on computer. It is based on the theoretical analysis of physical processes and parameters influencing the process to be modelled.

4.1. Mathematical modeling of the photovoltaic cell

Many models exist in the literature. The physical structure of a photovoltaic cell is similar to a diode whose PN junction is exposed to solar radiation. The models developed are based on an elementary electrical circuit including the effects of solar radiation and temperature variation on the photovoltaic cell [1].

A simple equivalent circuit of the PV cell consists of a current source in parallel with one or two diodes. The current is proportional to the illumination incident on the cell (photocurrent I_{PH}). The PV cell, in the dark, functions as a simple diode; if it is connected to an external source, it would produce an I_D current called Diode Current. The diode determines characteristic IV of the PV cell [1, 5-9].

To improve the model and consider its complexity and the losses generated in the cell and connections, the following modifications are made [7]:

- The dependence of the saturation current of diode I0 on temperature.
- The temperature dependence of the I_{PH} photocurrent.
- The RS serial resistance. It represents the internal losses due to the current being debited.
- The Shunt R_{SH} resistance, in parallel with the diodes. It corresponds to the leakage current to ground, it is often neglected
- The quality factor n of the diode will be considered variable (instead of being fixed at 1 or 2) or two diodes are introduced in parallel with Independent saturation currents.

a. Model of the photovoltaic cell with consideration of the losses of the series connections and in the diode

The photovoltaic cell is represented by a circuit equivalent to a diode in parallel to a voltage source varying according to solar radiation. This is the model of the PV cell with one diode usually used (Figure 5). The losses

due to the different connections are represented by the R_S resistance connected in series in this way, those due to the parasitic resistance in the diode are also considered; these losses are modelled in the equivalent circuit by the R_{SH} resistance. In shunt at the diode [2-3, 8-9].

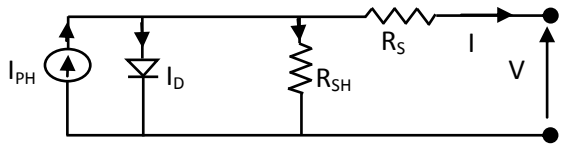

Figure 5: Circuit with a diode equivalent to the PV cell

We have:

$$\boldsymbol{I = I_{PH} - I_D - \frac{(V+IR_S)}{R_{SH}})} \quad \text{[Eq. 1]}$$

$$\boldsymbol{I_D = I_0\left(e^{\left(\frac{q}{nKT_C}(V+IR_S)\right)} - 1\right)} \quad \text{[Eq. 2]}$$

If we replace[Eq.9] in[Eq.8] we obtain :

$$I = I_{PH} - I_0\left(e^{\left(\frac{q}{nKT_C}(V+IR_S)\right)} - 1\right) - \frac{(V+IR_S)}{R_{SH}} \quad \text{[Eq. 3]}$$

The five parameters of this model are:

I_{PH} = photocurrent (A);

I_0 = reverse saturation current (A);

n = quality factor;

Rs = serial resistor (Ω) ;

R_{SH} = shunt resistor (Ω).

$V_{th} = \frac{K T_C}{q}$: thermodynamic potential.

I_D: diode current modelled by the equation of a Shockley diode (A);

q: electron charge (1.602×10^{-19} C) ;

K: Boltzmann constant (1.38×10^{-23} J/°K)

T_C: operating temperature of the PV cell (°K)

b. Simplification of the model with one diode

Simplifications are possible on the previous model. By neglecting the parasitic resistance in the diode, the circuit is reduced to a four-parameter circuit (the I_{PH} photocurrent; the inverse saturation current I_0; the quality factor n and the series Rs resistance) represented by figure 6.a [1, 8-9]. His equation becomes as follows [Eq. 4]:

$$\boldsymbol{I = I_{PH} - I_0\left(e^{\left(\frac{q}{nKT_C}(V+IR_S)\right)} - 1\right)} \quad \text{[Eq. 4]}$$

The losses due to the different connections can also be neglected in addition to the parasitic resistance in the diode. The ideal model of the photovoltaic cell in Figure 6.b with 3 parameters (the I_{PH} photocurrent; the reverse saturation current I_0 and the quality factor n) is shown. Its equation is simplified as follows [Eq. 5]:

$$\boldsymbol{I = I_{PH} - I_0\left(e^{\left(\frac{qV}{nKT_C}\right)} - 1\right)} \quad \text{[Eq. 5]}$$

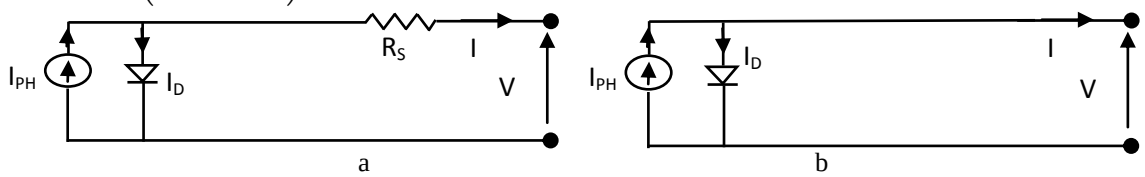

Figure 6: Simplification of the model has a diode: a) Model with 4 parameters; b) Model with 3 parameters

c. Model with two diodes, one series resistor and one parallel resistor

This model has two diodes and is more accurate in describing the PV cell. It consists of a voltage source varying according to the solar radiation, two diodes, a series resistor and a parallel resistor figure 7 [1, 8-9].
However, because of its implicit nature and non-linear form, it requires a high computing capacity.

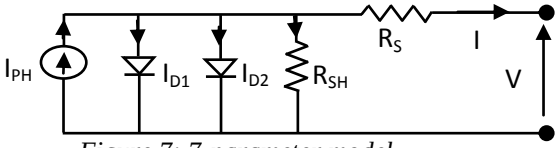

Figure 7: 7-parameter model

The equation [Eq.6] characteristic of this circuit is:

$$\boldsymbol{I = I_{PH} - I_{D1} - I_{D2} - \frac{(V+IR_S)}{R_{SH}}} \quad \text{[Eq. 6]}$$

With:

$$\boldsymbol{I_{D1} = I_{01}\left(e^{\left(\frac{q}{n_1 K T_C}(V+IR_S)\right)} - 1\right)} \quad \text{[Eq. 7]}$$

$$\boldsymbol{I_{D2} = I_{02}\left(e^{\left(\frac{q}{n_2 K T_C}(V+IR_S)\right)} - 1\right)} \quad \text{[Eq. 8]}$$

$$\boldsymbol{I = I_{PH} - I_{01}\left(e^{\left(\frac{q}{n_1 K T_C}(V+IR_S)\right)} - 1\right) - I_{02}\left(e^{\left(\frac{q}{n_2 K T_C}(V+IR_S)\right)} - 1\right) - \frac{(V+IR_S)}{R_{SH}}} \quad \text{[Eq. 9]}$$

The seven parameters of this circuit are:
I_{PH} = photocurrent (A);
I_{01} = inverse current of diode 1 saturation.
I_{02} = inverse current of diode 2 saturation.
$n_1 = A_1 \times (N_{CS})$, the quality factor of diode 1
$n_2 = A_2 \times (N_{CS})$, the quality factor of diode 2
A_1 et A_2: are the fulfillment factors for diodes 1 and 2.
N_{CS} = Number of cells in series.
Rs = serial resistor (Ω);
R_{SH} = shunt resistor (Ω).

d. Simplification of the dual diode model

On the previous model with two diodes we can consider that the parallel resistance is infinite [9], which reduces it to the model of figure 8.a with 6 parameters (the photocurrent I_{PH}; the saturation current of diode 1 I_{01}; the saturation current of diode 2 I_{02}; the quality factor of diode 1 $n_1 = A_1 \times N_{CS}$; the quality factor of diode 2 $n_2 = A_2 \times N_{CS}$ and the R_S series resistance with A_1 and A_2 the achievement factors of diodes 1 and 2 and NCS the Number of cells in series). The current-voltage relationship is given by the following equation [Eq. 10].:

$$\boldsymbol{I = I_{PH} - I_{01}\left(e^{\left(\frac{q}{n_1 K T_C}(V+IR_S)\right)} - 1\right) - I_{02}\left(e^{\left(\frac{q}{n_2 K T_C}(V+IR_S)\right)} - 1\right)} \quad \text{[Eq. 10]}$$

Assuming that the series resistance is negligible, the circuit is simplified as follows (figure 8.b)[9][12]. Neglecting the series resistance R_S in the equation (Eq.10), we obtain the following relationship (Eq.11):

$$\boldsymbol{I = I_{PH} - I_{01}\left(e^{\left(\frac{qV}{n_1 K T_C}\right)} - 1\right) - I_{02}\left(e^{\left(\frac{qV}{n_2 K T_C}\right)} - 1\right)} \quad \text{[Eq. 11]}$$

This model has five parameters (the photocurrent I_{PH}; the saturation current of diode 1 I_{01}; the saturation current of diode 2 I_{02}; the quality factor of diode 1 $n_1 = A_1 \times N_{CS}$ and the quality factor of diode 2 $n_2 = A_2 \times N_{CS}$ with A_1 and A_2 the achievement factors of diodes 1 and 2 and NCS the Number of cells in series).

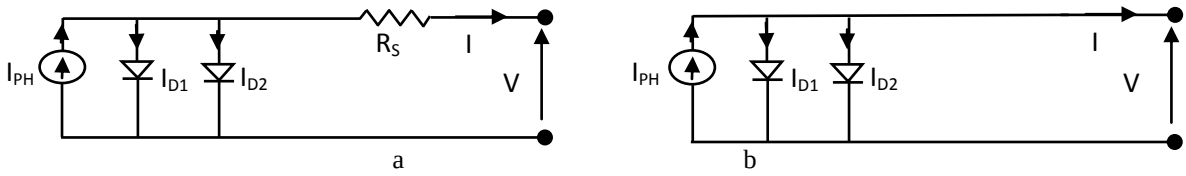

Figure 8: Simplification of the 2-diode model: a) Six-parameter model; b) Five-parameter model.

4.2. Effect of temperature on the photovoltaic generator

Several cell parameters (photocurrent, saturation current of the first diode, saturation current of the second diode, serial and parallel resistors...) depend on temperature [13]. The diode current increases as the temperature of the solar cells increases. The current of the solar panel being equal to the difference between the photocurrent and the diode current, there is a slight increase in the current Isc accompanied by a strong decrease in the Voc voltage and therefore a shift from the maximum power point Pmax to the lower powers [1, 7, 9-11].

Temperature coefficients highlight linear relationships between temperature and different electrical parameters of PV modules such as open-circuit voltage, maximum power point voltage and maximum power. They are provided by module manufacturers under STC conditions.

The photocurrent, related to illumination, temperature and photocurrent measured at reference conditions, is given by the equation (Eq.12): [9, 12-13]

$$I_{PH} = \frac{G}{G_{ref}}\left(I_{PH\_ref} + K_i\left(T_c - T_{c\_ref}\right)\right) \quad \text{[Eq. 12]}$$

With:

I_{PH}: photocurrent under reference condition [A]

K_i: sensitivity coefficient of intensity at temperature [A/K]

G ; G_{ref}: the actual illumination and at the reference condition [W/m²]

T_c ; T_{c_ref}: the actual cell temperature and at the reference condition

The reference photocurrent is defined by:

$$\boldsymbol{I_{PH\_ref}} = \frac{\boldsymbol{R_{SH}+R_S}}{\boldsymbol{R_{SH}}}\boldsymbol{I_{SC\_ref}} \quad \text{[Eq. 13]}$$

The saturation currents I_{01} and I_{02} are given by the following relationships (Eq.14) and (Eq.15): [13]

$$\boldsymbol{I_{01}} = \boldsymbol{I_{01\_ref}} * \left(\frac{\boldsymbol{T_C}}{\boldsymbol{T_{C_{ref}}}}\right)^{\boldsymbol{3}} * \boldsymbol{e}^{\left(\frac{\boldsymbol{q*E_g}}{\boldsymbol{Kn_1}}\left(\frac{\boldsymbol{1}}{\boldsymbol{T_{C_{ref}}}} - \frac{\boldsymbol{1}}{\boldsymbol{T_C}}\right)\right)} \quad \text{[Eq. 14]}$$

$$\boldsymbol{I_{02}} = \boldsymbol{I_{02\_ref}} * \left(\frac{\boldsymbol{T_C}}{\boldsymbol{T_{C_{ref}}}}\right)^{\frac{\boldsymbol{3}}{\boldsymbol{2}}} * \boldsymbol{e}^{\left(\frac{\boldsymbol{q*E_g}}{\boldsymbol{K\,n_2}}\left(\frac{\boldsymbol{1}}{\boldsymbol{T_{C_{ref}}}} - \frac{\boldsymbol{1}}{\boldsymbol{T_C}}\right)\right)} \quad \text{[Eq. 15]}$$

With I_{0_ref} given by;

$$\boldsymbol{I_{0\_ref}} = \frac{\boldsymbol{I_{SC\_ref}}}{\left(\boldsymbol{e}^{\left(\frac{\boldsymbol{V_{OC\_ref}}}{\boldsymbol{n\,V_{th\_ref}}}\right)}\right)-\boldsymbol{1}} \quad \text{[Eq. 16]}$$

With I_{01_ref} and I_{02_ref}, the reference saturation currents of the diodes, NOCT (Nominal Operating Cell Temperature) the nominal operating temperature of the cell, Eg energy of the semiconductor bandgap used in the cell, the ideality factor n depends on the technology used.

Influence of temperature on the open circuit voltage (Vco).

Experience shows that the open circuit voltage of a solar cell decreases with increasing cell temperature. A common order of magnitude of the loss is 2.3 mV/°C/cell. [10-11]:

The short-circuit current, on the other hand, increases slightly with the cell temperature (about 0.05% per degree Celsius).

The open circuit voltage depends mainly on the type of solar cell (PN junction, Schottky junction), the materials of the active layer and the nature of the contacts of the active-electrode layer. It also depends on the lighting of the cell [Eq. 17].

$$\boldsymbol{V_{OC} = \frac{K\,T_C}{q}\,log\left(\frac{I_{ph}}{I_S} + 1\right)} \quad \text{[Eq. 17]}$$

and Boltzmann's equation gives: $\boldsymbol{I_S = I_0 e^{\left(\frac{e\,V_0}{K\,T}\right)}}$ [Eq. 18]

With:

$V_{th} = \frac{K\,T_C}{q}$: representing the thermodynamic potential

T_C: is the absolute temperature

q: the electron charge constant, 1.602 10^{-19}.

K: the Boltzmann constant, 1.38 10^{-32},

I_{ph}: photocurrent

I_S: the saturation current

4.3. Matlab/Simulink modeling and simulation of the photovoltaic cell

For the modeling on Matlab/Simulink we had followed the following steps:

a) The temperature is generally given in degrees Celsius, it must be converted to degrees Kelvin (figure 10.a).

b) Determination of the reference saturation current of the diode by the equation (Eq. 16), (figure 10.b).

c) Figure 10.c shows the calculation of the photonic current Iph given by the equation (Eq. 12).

d) The saturation currents I_{01} and I_{02} which are given by the relationships (Eq.14) and (Eq.15) are modelled in Figures 11.a and Figures 11.b as follows.

e) Figure 12.a. shows the Simulink/Simscape model of diode 1 according to the equation (Eq. 7). Diode 2 is similar to diode 1 with the difference of determining the saturation current. Calculation of the diode current Id.

The photovoltaic cell (7-parameter model in Figure 7.) is modelled in Simulink/Simscape as follows in Figure 12.b.:

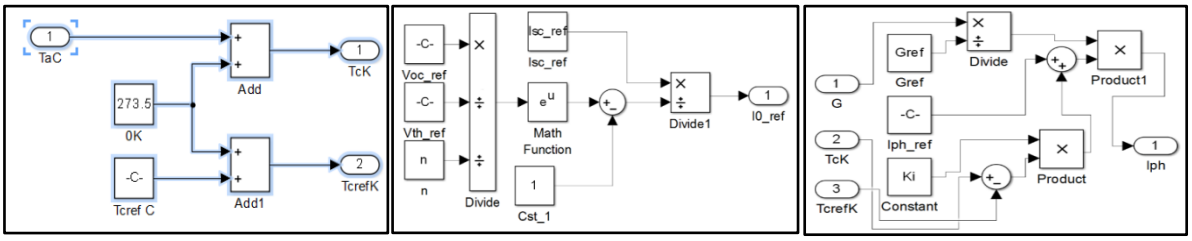

a b c

Figure 10: a) Temperature conversion circuit in degrees Kelvin. b) Circuit for calculating the reference saturation current. c) Calculation of the photonic current Iph

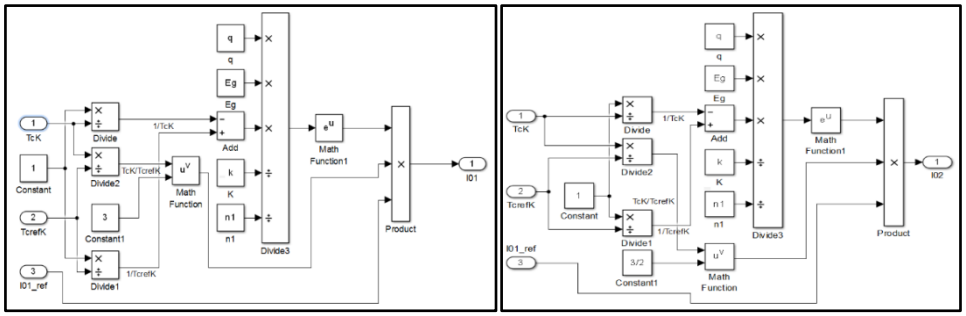

a b

Figure 11: Saturation current. a) Diode 1. b) Diode 2

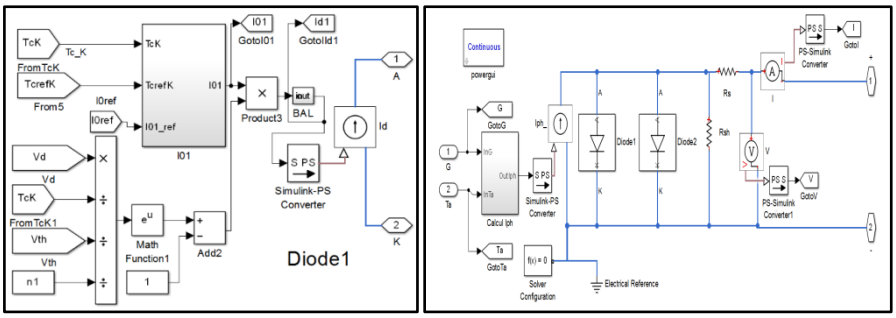

a b

Figure 12: a) Diode 1, determination of diode current I_D. b) Photovoltaic cell model in Simulink/Simscape.

Thus after the complete modeling we had put on the cell a variable resistive load as shown in Figure 13. :

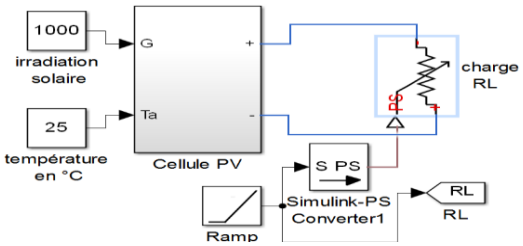

Figure 13: Photovoltaic cell model on a variable RL load

5. Simulation, results and interpretations

With the proposed model we extracted the different characteristics by varying the irradiation of the solar radiation.

5.1. Voltage/current and voltage/power characteristics for different irradiations

Figures 14.a and Figures 14.b show the general appearance of the electrical characteristics of a photovoltaic generator for different illuminations with fixed temperature (25°C).

We notice that, at a given temperature:

- the short-circuit current Icc varies in proportion to the illumination E ;
- the no-load voltage Vco varies little with illumination. It can be considered as a constant for a given installation;

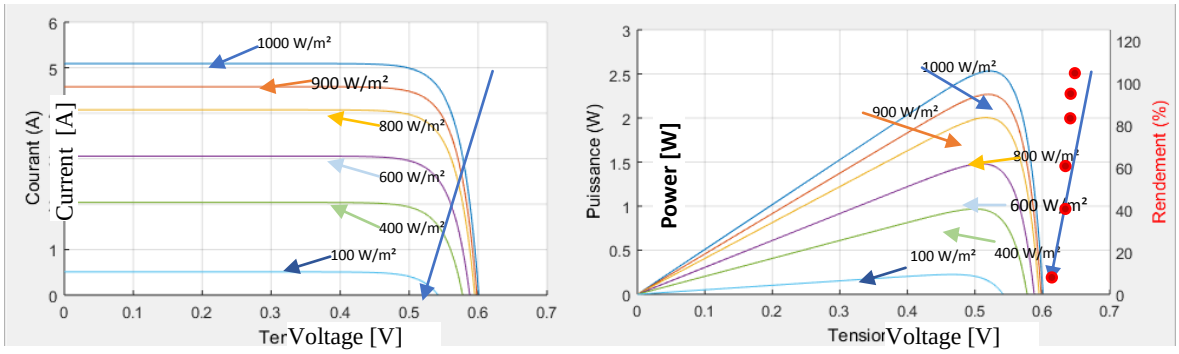

a b

Figure 14: PV characteristics for different irradiations; a) Current/Voltage IV characteristics. b) Power/Voltage characteristics

5.2. Voltage/current and voltage/power characteristics for different temperatures

Figures 15.a and Figures 15.b show the general appearance of the electrical characteristics of a photovoltaic generator for different temperatures with fixed illumination (1000 W/m²).

Let us note that when the temperature increases, Icc increases and Vco decreases.

The influences of these parameters therefore result in variations in the useful characteristic of the photovoltaic generator with lighting and temperature conditions, a phenomenon that must be taken into account when using it.

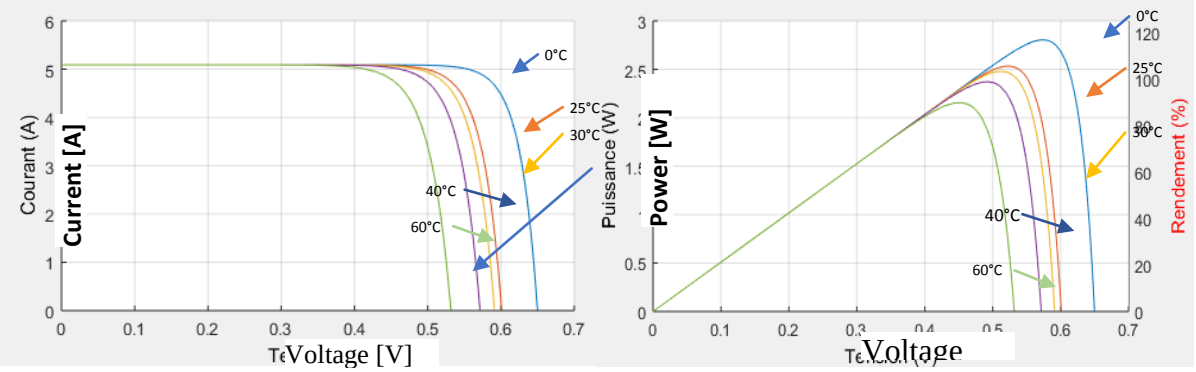

a b

Figure 15: PV characteristics for different temperatures. a) Current/Voltage characteristics IV. b) PV power/voltage characteristics.

6. Improved energy efficiency

For a load to operate on a PV generator, an operating point corresponding to the intersection of the two electrical characteristics must exist. For a direct connection of a resistive load R_l, (Figure 16.a). We had an example of a feature network in Figure 16.b.

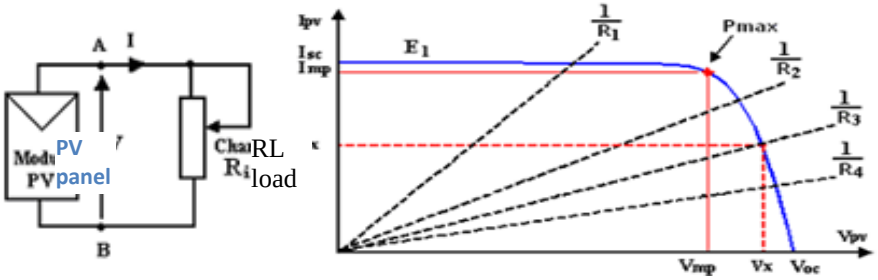

a) b)

Figure 16: Operating point. a) Direct electrical connection between a PV generator and a load. b) Operating points resulting from the association of PV generators under an illumination level E1 with a variable resistive load (R1, R2, R3, R4)

As can be seen in Figure 16.b, the working of the PV generator is highly dependent on the characteristics of the load with which it is associated.

Indeed, for a resistive load or, for any other load, of internal resistance Rl, the optimal power adaptation occurs only for a single particular operating point, named the Maximum Power Point (MPP) and noted in figure 16.b Pmax.

If the source-load operating point is not optimal, the performance of the assembly is not optimal. To significantly improve this efficiency, the photovoltaic generator will be connected to an electronic system that will allow the variation of the electrical operating point of the modules so that they operate optimally. The electronic system used to perform this function is the Maximum Power Point Tracker (MPPT). The MPPT is not a mechanical tracking system that "physically moves" the module for pointers directly on the sun. The two systems are different [14-16].

6.1. Converter

This MPPT role can be achieved by inserting a static DC/DC converter between the PV generator and the load. Its use allows the control of electrical power in DC circuits with very high flexibility and efficiency, ranging from 90 to 98%. They are composed of a power circuit and a control circuit implementing a tracking algorithm of the maximum MPP power point. As shown in Figure 17.a, at the DC/DC converter input is the PV row and at the output is the load [14, 16].

The DC/DC converter for MPPT can be designed based on the Buck or Boost chopper.
The Buck converter is used to lower the output voltage and the Boost converter (Figure 17.a) to obtain higher output voltages [17].

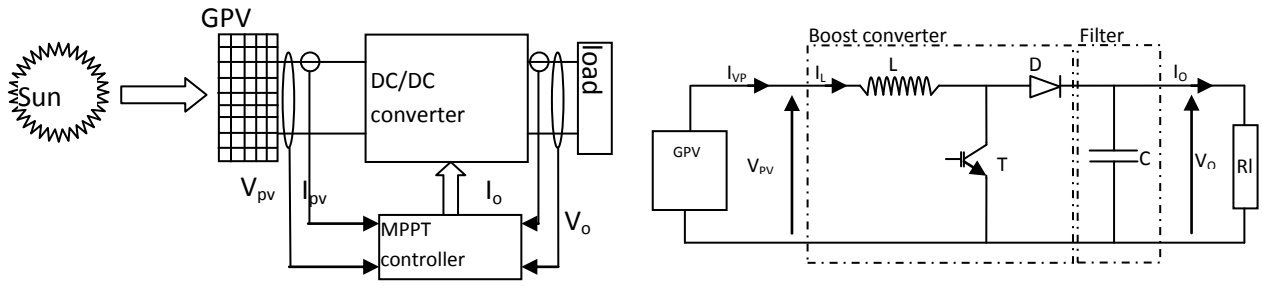

a b

Figure 17: MPPT principle: a) Photovoltaic conversion element chain controlled by a MPPT; b) Boost converter

Despite the high inherent efficiency of the Buck converter in systems with conventional power sources, the Boost converter (Figure 17.b.) may be more suitable for photovoltaic systems with the Maximum Power Point Tracker (MPPT) since the converter operates in direct current mode extracting as much power as possible from the solar cells. Therefore, the energy efficiency of the Boost converter may be greater than that of the Buck converter [14].
The transformation ratio is, by calling α the duty cycle (ratio of the time during which the transistor is closed, to the hash period):

$$\frac{V_{VP}}{V_O} = \frac{1}{1-\alpha} \qquad \text{[Eq. 19]}$$

6.2. MPPT principle et algorithm

Several algorithms for determining the MPP exist. The PO (Disruption and Observation) method is simple and easy to implement to perform an MPP search. This technique is available in several variants for its implementation. It consists in calculating the MPP by iteration. It measures the PPV power on the panels, then disrupts the operating point to detect the power variation. If the power increases, the system continues in this direction, but if it decreases the direction of the disturbance is reversed. When the MPP is reached the system oscillates around the maximum power measured PPV, The algorithm of this technique is given in Figure 18 and Figure 19 [18-19].
Most modern MPPT controllers can achieve efficiencies between 92% and 98%.
Actual gains may vary widely depending on weather, temperature, state of charge and other factors.

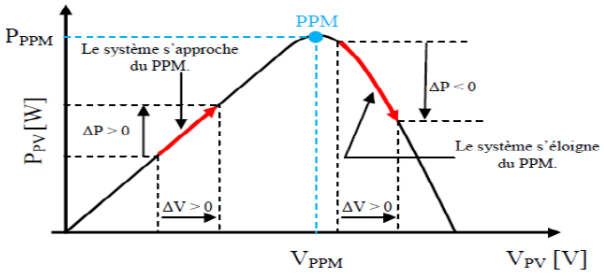

Figure 18: Principle of Maximum power point tracking

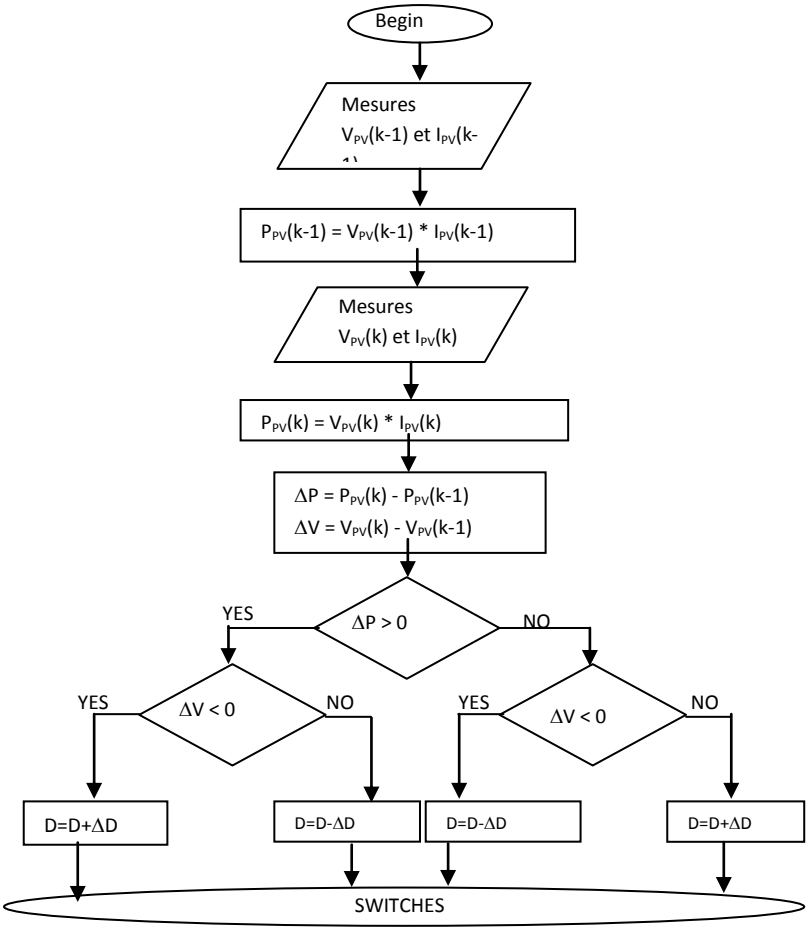

Figure 19: PO algorithm "Perturbation and Observation"

6.3. MPPT Modeling

The MPPT system consists of two components: the PO control and the Boost chopper.

The development of the control according to the PO algorithm (Disruption and Observation) is shown in Figure 20.a. The switch control logic signals depend on the type of converter used; an PWM (Pulse Width Modulation) command will be used.

An implementation, on SimPowerSystems (Matlab), of the Boost chopper, according to the diagram in Figure 17.b, is given below (Figure 20.b),

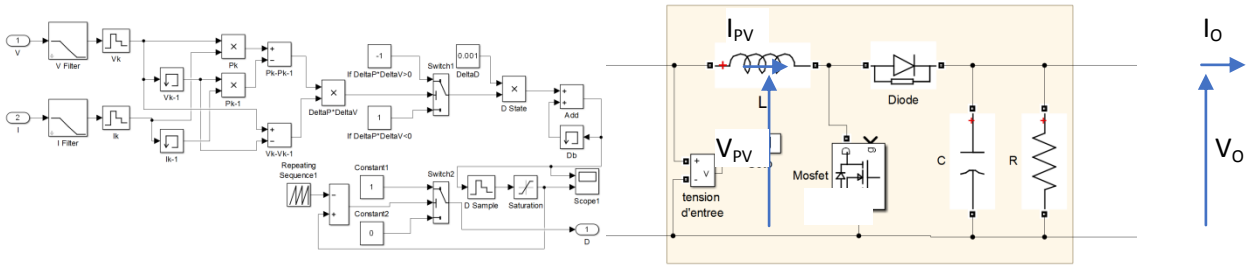

a b

Figure 20: MPPT modeling on Simulink and SimPowerSystem: a) PO algorithm (Perturbation and Observation); Boost chopper (without control)

6.4. Simulation, results and interpretations of the Boost

The results are given by varying the solar radiation and temperature. For the following simulation the PV source has the following characteristics:

Voc = 37,6 V (60 cells in series).
Isc = 8,55 A
Tk = 25 °C
Vmp = 31 V
Imp = 8,06 A

The characteristic curves and models are shown in the following figures 21.a, figures 21.b, figures 22.a and figures 22.b :

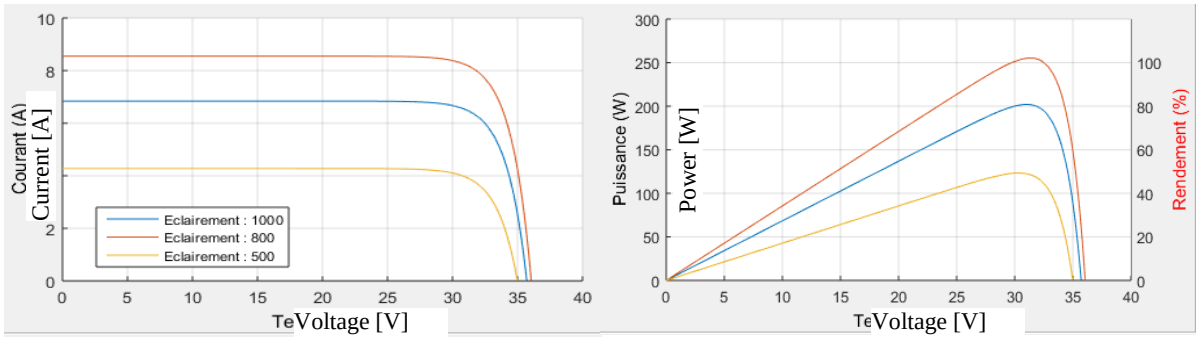

a b

Figure 21: Characteristic of the PV source. a) Characteristic VI b) P-V characteristic

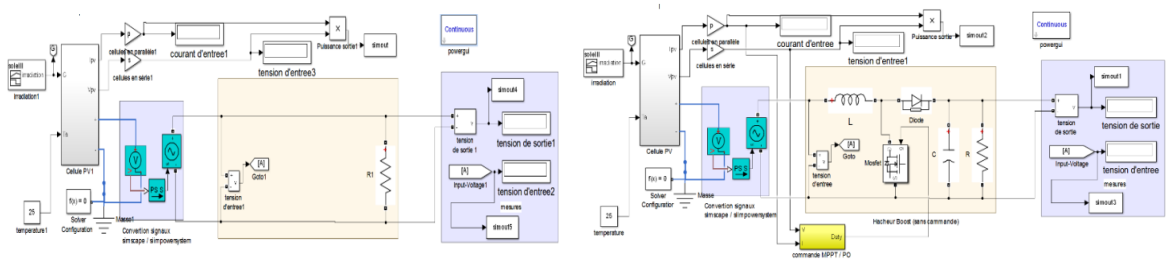

a b

Figure 22: Simulated system. a) without MPPT. b).with MPPT

The results of the simulation, under 25°C with a load of 30 Ω, powered by a photovoltaic source with and without the MPPT system, are presented below.

The measurements obtained (Table 1), in a first phase, were carried out with 500W/m², 800W/m² and 1000W/m² sunlight (Figure 23.).

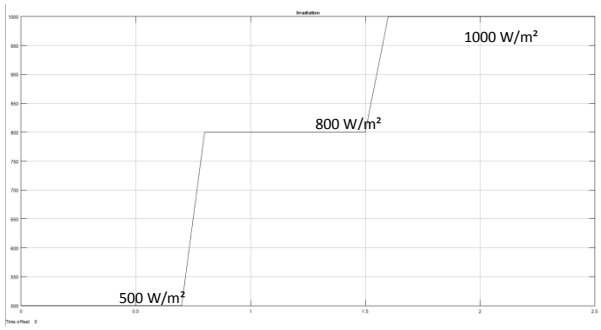

Figure 23: Variation in sunlight

Under the three sunlight conditions we see a significant improvement in the power supplied by the PV system. We had a power gain of 121% under 500 W/m², 273% under 800W/m² and 336% under 1000W/m² (Table 1.). The curves describing the instantaneous variations in power and voltage are given in Figures 24.a and Figures 24.b.

Under the three conditions the Boost converter to achieve an efficiency greater than 0.92.

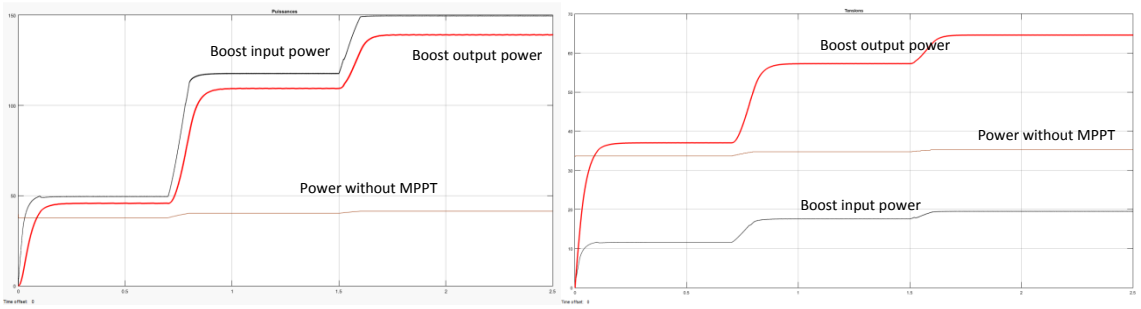

a b

Figure 24: Variation according to sunshine. a) Power variation. b) Voltage variation

For the second measurement phase the simulation, under the following conditions; an insolation of 1000W/m², a load of 30 Ω and three temperature levels (25°C, 30°C and 45°C Figure 25.). The load is always powered by a photovoltaic source with and without the MPPT system. The results are obtained as shown in Table 2 and Figures 28.

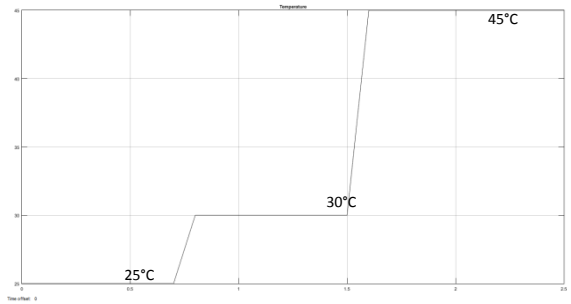

Figure 25: Temperature variation pattern

Under the irradiation of 1000W/m² and by varying the temperature, there is always an improvement in the power supplied by the PV system using the MPPT system. We had a power gain of 336% under 25°C, 345% under 30°C and 350% under 45°C, (Table 2.).

Unlike the previous simulation, the power decreases with temperature, which was predictable. The curves describing the instantaneous variations in power are given in Figure 28.

Under the three conditions the Boost converter to achieve an efficiency of about 0.93.

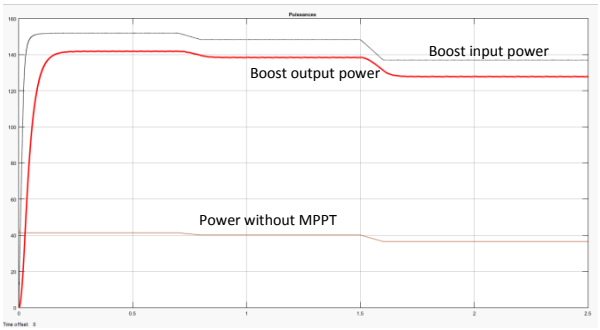

Figure 28: Power variation with temperature.

In both simulation series we had a significant improvement in the power supplied by the PV system. But the converter used here is of the Boost type, voltage booster type; the efficiencies will not be improved if the operating point voltage is lower than the optimal PV voltage.

Table 1: Results of the PV System by varying the irradiation

Temperature 25°C / Load resistance 30 Ω					
Irradiation		**PV Voltage**	**PV Power**	**Load power**	**Boost efficiency**
500 W/m²	With MPPT	11,6 V	49,59 W	45,73 W	0,92
	Without MPPT	33,62 V	37,68 W	37,68 W	
	Gain			8,05 W / 121%	
800 W/m²	With MPPT	17,54 V	117,5 W	109,3 W	0,93
	Without MPPT	34,74 V	40,22 W	40,22 W	
	Gain			69,08 W / 273%	
1000 W/m²	With MPPT	19,53 V	149,7 W	139,2 W	0,93
	Without MPPT	35,23 V	41,37 W	41,37 W	
	Gain			97,83 W / 336%	

Table 2: PV System results by varying the temperature

Irradiation 1000 W/m² - Load resistance 30 Ω					
Temperatures		**PV Voltage**	**PV Power**	**Load power**	**Boost efficiency**
25°C	With MPPT	19,53 V	149,7 W	139,2 W	0,93
	Without MPPT	35,23 V	41,37 W	41,37 W	
	Gain			97,83 W / 336%	
30°C	With MPPT	20,38 V	148,3 W	138,3 W	0,93
	Without MPPT	34,70 V	40,14 W	40,14 W	
	Gain			98,16 W / 345%	
45°C	With MPPT	19,6 V	137 W	127,8 W	0,93
	Without MPPT	33,11 V	36,55 W	36,55 W	
	Gain			91,25 W / 350%	

7. Conclusions

Simulation is a very effective tool for studying and predicting physical and non-material systems. In this paper we had modelled the photovoltaic cell. The implementation of the described models is quite easy with modeling and simulation software such as MATLAB/ SIMULINK / SIMSCAPE.

The simulation highlighted the non-linear characteristics of the PV cell under different environmental conditions.

The interest of an optimization stage was also highlighted. The proposed model demonstrated the merits of using an MPPT system for a more optimal use of the PV source.

On the other hand, the use of other types of converters (BUCK, CUK, BUCK-BOOST...) and other MPPT algorithms (incremental conductance (INC), parasitic capacitance (PC), constant voltage (CV)...) could allow a more advanced study of the subject.

Acknowledgements

My thanks go to Prof. Amadou SAIDOU MAIGA who supported us to finalize our work.

References

[1]. Antonio L., Steven H. "Handbook of Photovoltaic Science and Engineering "John Wiley & Sons Ltd, The Atrium, Southern Gate, Chichester, West Sussex PO19 8SQ, England, 2003.

[2]. A. Shukla, M. Khare, K. N. Shukla, "Modeling and Simulation of Solar PV Module on MATLAB/Simulink" International Journal of Innovative Research in Science, Engineering and Technology , IJIRSET , Vol. 4, Issue 1, January 2015, ISSN (Online): 2319 – 8753 ISSN (Print): 2347 – 6710.

[3]. M. U. Olanipekun, A. J. Olanipekun, K. A. Amusa , A. J. Opeodu, "Parameters extraction of a double-diode model of photovoltaic cell using newton-raphson method", FULafia Journal of Science &

Technology Vol. 4 Special Edition, September 2018, ISSN (Print): 24490954 , ISSN (Online): 26364972.

[4]. K. Ranabhat, L. Patrikeev, A. A. Revina, K. Andrianov, V. Lapshinsky, E. Sofronova, "AN Introduction to Solar Cell Technology" Review Paper iipp, doi:10.5937/jaes14-10879 Paper number: 14(2016)4, 405, 481–491.

[5]. Jean-Claude Muller, "Électricité photovoltaïque - Principes", Techniques de l'Ingénieur, dossier [BE8578], base documentaire : Archives énergie (1992).

[6]. Ludovic Protin, Stéphan Astier, "Convertisseurs photovoltaïques", Techniques de l'Ingénieur, dossier [D3360], base documentaire : traité Génie électrique (1992).

[7]. Amrita Mantri, Dr. Ajay Verma, "Simulink Models of PV Array under Varying Conditions'', Volume-5, Issue-1, February-2015 International Journal of Engineering and Management Research Page Number: 69-74, ISSN (Online): 2250-0758, ISSN (Print): 2394-6962.

[8]. V. Tamrakar, S.C. Gupta, Y. Sawle, "Single-diode and two-diode pv cell modeling using matlab for studying characteristics of solar cell under varying conditions", Electrical & Computer Engineering: An International Journal (ECIJ) Volume 4, Number 2, June 2015, doi : 10.14810/ecij.2015.4207 67

[9]. Helali Kamelia, "Modélisation D'une Cellule Photovoltaïque: Etude Comparative", Mémoire de Magister En Electrotechnique, UMMTO (Tizi-Ouzou), 2012.

[10]. M. Shrestha, N. Bhattarai, "Impact Study on Power Generation from Photovoltaic System due to Change in Local Irradiance and Temperature at Kathmandu Valley, Nepal", Journal of the Institute of Engineering, 2016, 12(1): 1-9 © TUTA/IOE/PCU Printed in Nepal.

[11]. M. Abderrezek, M. Fathi, S. Mekhilef, F. Djahli "Effect of Temperature on the GaInP/GaAs Tandem Solar Cell Performances", International Journal of Renewable Energy Research Vol.5, No.2, 2015.

[12]. Snehamoy Dhar, R Sridhar, Varun Avasthy, "Modeling and Simulation of Photovoltaic Arrays'', Department of Electrical & Electronics Engineering, SRM University, Chennai.

[13]. Md. W. Shah, Robert L. Biate, "Design and Simulation of Solar PV Model Using Matlab/Simulink ", International Journal of Scientific & Engineering Research, Volume 7, Issue 3, March-2016 ISSN 2229-5518.

[14]. S. L. Lyden, "A Simulated Annealing Global Maximum Power Point Tracking Method for Photovoltaic Systems Experiencing Non-Uniform Environmental Conditions" B.Sc-B.E (Hons), Doctor of Philosophy, University of Tasmania, June 2015.

[15]. A. Sfirat, A. Gontean, S. Bularka, "A New Method for MPPT Algorithm Implementation and Testing, Suitable for Photovoltaic Cells", Advances in Electrical and Computer Engineering Volume 18, Number 3, 2018 , DOI 10.4316/AECE.2018.03008.

[16]. Henri Foch et al., "Conversion continu-continu - Hacheurs'', Editions Techniques Ingénieurs, dossier [D3160], 2003.

[17]. Wildi T., Sybille G., 2005. "Electrotechnique'', 4e Edition, ISBN DBU 2-8041-4892-0. De Boeck, Paris.

[18]. T.R. Premila and R. Krishna Kumar "A Comprehensive Review on Various Optimization Techniques Assisted Perturb and Observe MPPT Algorithm for a PV System" , International Journal of Pure and Applied Mathematics , Volume 118 No. 5 2018, 51-63, ISSN: 1311-8080 (printed version); ISSN: 1314-3395 (on-line version), url: http://www.ijpam.eu , Special Issue

[19]. S. Selvan, P. Nair, Umayal, "A Review on Photo Voltaic MPPT Algorithms", International Journal of Electrical and Computer Engineering (IJECE), Vol. 6, No. 2, April 2016, pp. 567-582, ISSN: 2088-8708, doi: 10.11591/ijece.v6i2.9204.